



A robust walking detection algorithm using a single foot-worn inertial sensor: validation in real-life settings

Gaëlle Prigent¹ · Kamiar Aminian¹ · Andrea Cereatti^{2,3} · Francesca Salis^{3,4} · Tecla Bonci⁵ · Kirsty Scott⁵ · Claudia Mazzà⁵ · Lisa Alcock⁶ · Silvia Del Din⁶ · Eran Gazit⁷ · Clint Hansen⁸ · Anisoara Paraschiv-Ionescu¹ · for the Mobilise-D consortium

Received: 26 September 2022 / Accepted: 8 March 2023
© The Author(s) 2023

Abstract

Walking activity and gait parameters are considered among the most relevant mobility-related parameters. Currently, gait assessments have been mainly analyzed in laboratory or hospital settings, which only partially reflect usual performance (i.e., real world behavior). In this study, we aim to validate a robust walking detection algorithm using a single foot-worn inertial measurement unit (IMU) in real-life settings. We used a challenging dataset including 18 individuals performing free-living activities. A multi-sensor wearable system including pressure insoles, multiple IMUs, and infrared distance sensors (INDIP) was used as reference. Accurate walking detection was obtained, with sensitivity and specificity of 98 and 91% respectively. As robust walking detection is needed for ambulatory monitoring to complete the processing pipeline from raw recorded data to walking/mobility outcomes, a validated algorithm would pave the way for assessing patient performance and gait quality in real-world conditions.

Keywords Walking detection · Real-world · Foot-worn sensor · Continuous wavelet transform · Adaptive threshold

✉ Gaëlle Prigent
gaelle.prigent@epfl.ch

Kamiar Aminian
kamiar.aminian@epfl.ch

Andrea Cereatti
acereatti@uniss.it

Francesca Salis
fsalis1@uniss.it

Tecla Bonci
t.bonci@sheffield.ac.uk

Kirsty Scott
k.scott@sheffield.ac.uk

Claudia Mazzà
c.mazza@sheffield.ac.uk

Lisa Alcock
lisa.alcock@ncl.ac.uk

Silvia Del Din
Silvia.Del-Din@newcastle.ac.uk

Eran Gazit
erang@tlvmc.gov.il

Clint Hansen
c.hansen@neurologie.uni-kiel.de

- ¹ Laboratory of Movement Analysis and Measurement (LMAM), École Polytechnique Fédérale de Lausanne, Lausanne, Switzerland
- ² Department of Electronics and Telecommunications, Politecnico Di Torino, Turin, Italy
- ³ Department of Biomedical Sciences, University of Sassari, Sassari, Italy
- ⁴ Interuniversity Centre of Bioengineering of the Human Neuromusculoskeletal System, Sassari, Italy
- ⁵ Department of Mechanical Engineering and Insigneo Institute for in Silico Medicine, University of Sheffield, Sheffield, UK
- ⁶ Translational and Clinical Research Institute, Faculty of Medical Sciences, Newcastle University, Newcastle Upon Tyne, UK
- ⁷ Center for the Study of Movement, Cognition and Mobility, Neurological Institute, Tel Aviv Sourasky Medical Center, Tel Aviv, Israel
- ⁸ Department of Neurology, University Medical Center Schleswig-Holstein Campus Kiel, Kiel, Germany

1 Introduction

The use of wearable sensors offers a valuable opportunity to obtain objective and valid mobility data in free-living conditions [1, 2]. Walking activity and gait parameters are considered among the most relevant mobility-related parameters [3, 4]. Gait speed has been referred to as the sixth vital sign [5] and has been shown to be a reliable marker of functional decline and mobility [6, 7]. The assessment of walking in real-life conditions and the effects of specific interventions or medications on patient mobility are hence of great interest [8]. In this context, automatic detection of walking bouts (WBs) (also referred as to gait/walking periods) before further gait analysis and speed estimation is necessary.

The most commonly used algorithms for ambulatory locomotion detection are based on trunk-mounted (chest/lower back) inertial measurement units (IMUs) and use different approaches such as threshold-based methods [9–12], zero-crossing methods [13, 14], and pattern recognition [15]. One of the main advantages of using a sensor on the chest/lower back is the possibility to detect other physical activities besides locomotion, such as lying, sitting, standing, and postural transitions [16–18]. The advantage of lower back position is the estimation of step length, cadence and gait speed [19]. A wrist-mounted sensor is also commonly used to assess daily activity [20–22] because it is practical to use and convenient for participants. Although recent algorithms allow estimation of gait speed based on lower back or wrist position [23, 24], a foot/shank-mounted IMU may provide detailed spatio-temporal parameters with clinically acceptable accuracy [25, 26]. This is because the assumption of zero-velocity-update can be exploited to reduce errors affecting the estimation of spatial parameters [25, 27–29].

In a systematic review, Vienne et al. [2] identified seven clinical criteria for semiological descriptions of gait quality in patients with neurological disorders, i.e., springiness, sturdiness, smoothness, steadiness, stability, symmetry, and synchronization [2]. With the exception of stability and synchronization, requiring an IMU attached to the trunk, all the other gait criteria can be computed from an IMU attached to the shank or foot. Therefore, in the context of clinical studies, in which accurate locomotion identification and detailed gait analysis are critical for outcome evaluation, the foot can be considered as an appropriate sensor location.

Currently, gait assessments have been mainly analyzed in laboratory or hospital settings [2]. In a systematic review, Vienne et al., 2017 reported that of the 78 included studies, only 9 examined gait when patients were in their natural home environment, and only one measured gait with a foot-worn sensor. Recently, discrepancies have been demonstrated

in mobility parameters measured in unsupervised and in laboratory settings [30]. Short walking tests performed in the laboratory provide a snapshot of patients' capacity, which does not reflect their usual performance (i.e., real world behavior). There is growing consensus that unsupervised assessments for long-term mobility evaluation in real-life conditions can complement supervised walking tests, and contribute to individualized clinical decisions [30, 31]. The main challenge in unsupervised measurements is the need for an accurate gold standard reference system for algorithm validation. Video recordings are often used as a reference for labelling real-life activities [32]. However, manual labelling is very time-consuming, cumbersome, and should be performed independently by multiple observers to allow for cross-validation. Recently, a multi-sensor wearable system, which integrates pressure insoles with multiple IMUs and infrared distance sensors (INDIP), have been developed to be used as references for real-world experimentation and locomotion detection [33, 34]. Instrumented insoles, combined with IMUs, provide reliable identification of initial and final foot contacts, which is essential for walking bout detection and gait analysis [33].

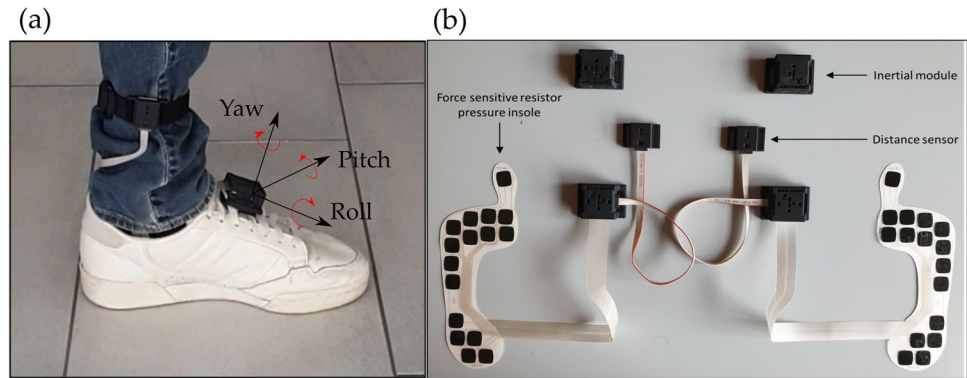
Given the above-mentioned considerations, a robust detection of walking bouts for ambulatory monitoring based on foot-mounted IMUs is necessary to complete the processing pipeline from raw recorded data to walking/gait-related mobility outcomes. A validated algorithm would pave the way for evaluating patient performance and gait quality in a natural home environment. Therefore, using the INDIP pressure sensor system as a reference, the aim of this study is to validate a walking bout detection algorithm using data recorded in real-life like environments with a foot-mounted IMU. The algorithm was evaluated for various sensor configurations, i.e., for one IMU (one foot) or two IMUs (two feet), and for 3D acceleration or 3D angular velocity signals.

2 Methods

2.1 Materials and data collection

Data used to evaluate the performance of the proposed WBs detection algorithm were recorded in 18 healthy subjects (10 healthy young (HY) and 8 healthy adults (HA)) who performed 2.5 h of free-living activities. The study was approved by the University of Sheffield Research Ethics Committee (application number 029143). During the 2.5 h of measurement, subjects were asked to: (1) rise from a chair and walk to another room; (2) walk to the kitchen and make a drink; (3) walk up and down a set of stairs; (4) walk outside, if possible for a minimum of 2 min; and (5) if walking outside, walk up

Fig. 1 Multi-sensor wearable system (INDIP); (a) INDIP system attached on the shoe, and (b) picture of two INDIP sensors (right and left feet), which integrate force sensitive resistor pressure insoles, inertial modules (IMUs), and infrared distance sensors



and down an inclined path. Each participant was equipped with a INDIP wearable multi-sensor system (Fig. 1). The INDIP system includes on each foot an IMU (3D accelerometer, ± 16 g; 3D gyroscope, ± 2000 dps; 3D magnetometer), 2 distance sensors, and two 16-elements plantar pressure insoles. In this study, acceleration and angular velocity, recorded at 100 Hz from shoe-mounted IMUs, were used to develop a new algorithm for step/stride and WBs detection. The performance of this algorithm was validated using the INDIP system, and dedicated algorithms, as a reference (ground truth) [33].

2.2 Algorithm implementation

Step or stride detection from foot-worn sensors are generally based on the detection of peaks associated to consecutive mid-swing, heel-strike [28] or toe-off [35] instants in the pitch angular velocity obtained from the gyroscope signal. However, those detections are highly sensitive to sensor placement and orientation, and require a calibration procedure [25]. Thus, in this study, the 3D angular velocity norm, (ωN , Eq. 1) is used to overcome the calibration step:

$$\omega N = \sqrt{\omega_{roll}^2 + \omega_{pitch}^2 + \omega_{yaw}^2} \quad (1)$$

where ω_{roll} , ω_{pitch} and ω_{yaw} are the components of the angular velocity signal recorded by the gyroscope around the 3D rotation axes. In addition to the gyroscope signal, we also tested the performance of the algorithm when using the acceleration norm (aN) as input, making our methodology usable for 3D accelerometer only.

When using one IMU on one foot, only stride-related information from the instrumented foot can be extracted. The acceleration and angular velocity norm demonstrate periodic patterns with peaks generated by the contact with ground (i.e., heel-strike and toe-off) and the mid-swing events at each stride. To enhance these periodic patterns and reduce the effect of movement artefacts, a *peak enhancement* stage was applied to obtain a signal

containing stride-related information. Then, a *peak selection* stage using threshold-based approaches was designed to select the peaks corresponding to the strides [36]. A similar approach was used when considering two IMUs (one on each foot) to obtain step-related information. Finally, a *walking bout detection* method was applied using the selected strides or steps (Fig. 2). In the following paragraphs, we described these three stages with ωN used as the input signal.

2.2.1 Peak enhancement

The objective of this first stage is to obtain a signal that contains improved stride-related information. This peak enhancement method should be robust to various gait patterns/impairments. The raw angular velocity norm (ωN) is first down-sampled to 40 Hz to decrease the processing time when data is recorded in long-term monitoring protocols. Then, the signal is detrended and low-pass filtered (FIR filter, $n = 120$ coefficients, cutoff frequency: $F_c \approx 3.2$ Hz) to obtain $\omega N-LPF$ [10]. The cutoff frequency F_c was chosen to smooth the signal by removing the high frequency noise. As FIR filters have a linear phase shift, the shape of the waveform is not modified, however, a delay is introduced. To eliminate the delay and obtain zero-phase distortion, the filter is applied to ωN twice using the Matlab function *Filtfilt*. Subsequently, the continuous wavelet transform (cwt, scale 15, gauss2 wavelet in Matlab) is used as a smoothing and differentiation procedure [37], allowing a stride-related peaks enhancement consistent among various impaired or atypical gait patterns. The cwt time-scale was set to 15 to be adapted to stride detection. Finally, additional slight smoothing is performed using a linear Savitzky-Golay filter. The processed signal is referred to as $\omega N-LPF-CWT$. An illustrative example of the peak enhancement procedure for the signals recorded from one-foot IMU is shown in Fig. 3, and in Supplementary material A when two IMUs are used (one on each foot).

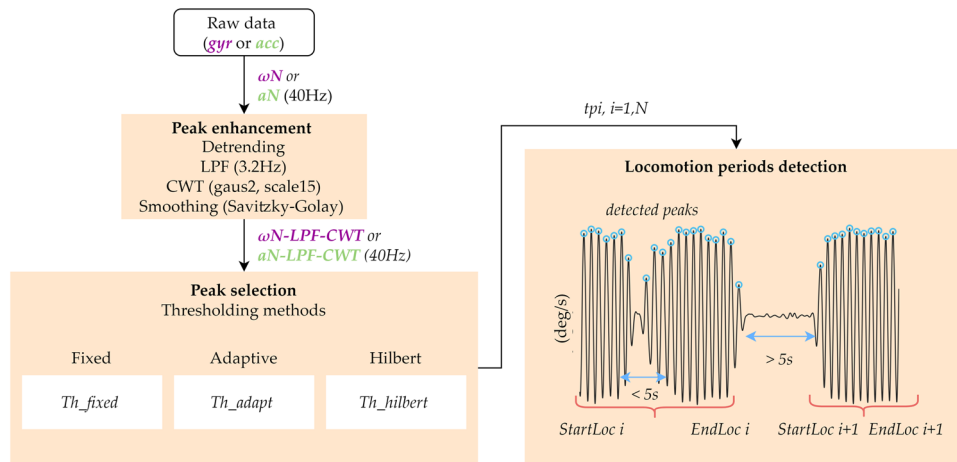


Fig. 2 Flowchart of the walking bouts detection algorithm for one-foot IMU. ωN : raw angular velocity norm; aN : raw acceleration norm; LPF: low-pass filter; CWT: continuous wavelet transform; TH_{fixed} : fixed threshold ($TH_{fixed} = 100\text{deg/s}$ or $TH_{fixed} = 0.5\text{g}$); TH_{adapt} : adaptive threshold based on the percentile of the obtained

amplitude distribution of peaks detected above the fixed threshold (TH_{fixed}); $TH_{hilbert}$: Hilbert threshold based on the Hilbert envelope and percentile of the obtained amplitude distribution of peaks detected; tp_i : time of peak occurrence; $StartLoc\ i$: start of the walking bout i ; $EndLoc\ i$: end of the walking bout i

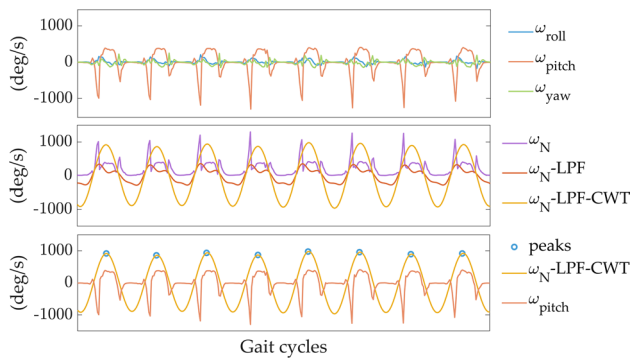


Fig. 3 Angular velocity signals recorded with the 3D gyroscope on one foot during several gait cycles for one subject. The top panel shows the raw angular velocity signals around the three axes (roll, pitch, yaw). The middle panel shows the raw angular velocity norm (ωN , magenta), the signal after detrending and LPF ($\omega N-LPF$, red), and the signal after continuous wavelet transform ($\omega N-LPF-CWT$, yellow). The bottom panel shows the pitch angular velocity, the continuous wavelet transform ($\omega N-LPF-CWT$, yellow), and the detected strides. Strides are identified as maxima corresponding to mid-swing events (blue circle) with an amplitude higher than a certain threshold (TH_{fixed} , TH_{adapt} , or $TH_{hilbert}$)

2.2.2 Peak selection

From the processed gyroscope angular velocity signal ($\omega N-LPF-CWT$, Fig. 2), the time of occurrence tp_i of each peak (p_i) with amplitudes higher than a specific threshold are selected as potential stride-related temporal events. These peaks (p_i) correspond to mid-swing events when the gyroscope norm is used as input. The heel-strike events, on the other hand, are detected when

the acceleration norm is used. Three amplitude thresholding methods were implemented and tested in this study. The first method is based on a fixed threshold $TH_{fixed} = 100(^{\circ}/s)$, ($TH_{fixed} = 0.5\text{g}$), when the acceleration is used as input signal). Both thresholds were chosen in a conservative manner to allow detection of stride-related temporal events for a wide range of walking speeds [38]. The second approach relies on an adaptive threshold (TH_{adapt}) based on the percentile of the obtained amplitude distribution of peaks detected above the fixed threshold (TH_{fixed} , Fig. 4). Finally, in the third method, we applied the Hilbert transform to pre-select potential walking bouts. The Hilbert envelope of the filtered signal $\omega N-LPF-CWT$ is computed for a pre-selected of potential walking periods [39]. Then, the threshold ($TH_{hilbert}$) is defined as the percentile of the amplitude distribution of all peaks in the pre-selected bouts (Fig. 4). Percentile values from 1 to 50%, with increment of 2.5%, were tested through receiver operating characteristic curve (ROC) for the two adaptive thresholding methods.

Figure 4a–b shows the filtered signal $\omega N-LPF-CWT$ and the derived thresholds TH_{adapt} (blue) and $TH_{hilbert}$ (purple), as well as the selected peaks (dark dots with amplitude above the thresholds), for data recorded in one subject. Figure 4c shows the amplitude distributions of the peaks and the thresholds obtained for each of the three methods tested (fixed, adaptive and Hilbert). The fixed-threshold TH_{fixed} is lower than the other two because it is less restrictive. In contrast, the adaptive threshold $TH_{hilbert}$ is higher because of the pre-selected walking periods (dashed line in Fig. 4b).

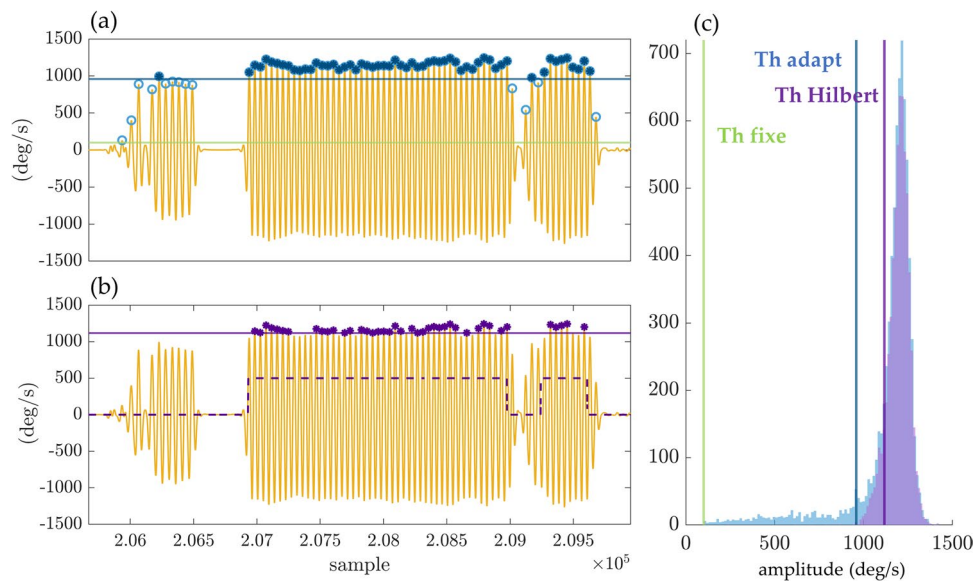


Fig. 4 Thresholding methods for peak selection, example based on data from one subject: **(a)** the filtered signal ωN -LPF-CWT (orange) is shown, as well as the obtained TH_{adapt} (dark blue) and the selected peaks (dark blue starts with amplitudes above the thresholds); **(b)** the Hilbert envelope method is shown with the preselected walking periods (dashed line), and the selected peaks (dark purple dots); **(c)**

amplitude distributions of the peaks, and the thresholds obtained for each of the three tested methods (TH_{fixed} (green), TH_{adapt} (blue) and $TH_{hilbert}$ (purple)). The histograms of the peaks obtained for the *fixed* and *adaptive* thresholds are identical. In fact, TH_{adapt} is defined as the 10th percentile of the distribution obtained after applying the fixed-threshold $TH_{fixed} = 100^\circ/s$

2.2.3 Strides and walking bouts detection using one IMU (one foot)

The next stage consists of detecting the actual strides from peaks p_i and identifying the beginning/end of the walking periods. Successive peaks with duration $\Delta t_i = tp_{i+1} - tp_i$ ($i = 1, N - 1$) lower than the adaptive *duration threshold* (TH_d) are considered as part of the same walking period. When one IMU is used, the threshold TH_d is initialized with a fixed value of 5 s. Then, the threshold is updated at each iteration using the formula $TH_d = 3 + average(Dstride)(s)$, with $Dstride$ defined as the average duration of the previous strides that belong to the current WB. TH_d is designed to adapt to the cadence of the current walking period, which improves the robustness of the stride detection under real-life conditions. The algorithm is also designed to be resilient to short breaks or occasional undetected stride-related peaks (e.g., during turning, gait asymmetry) by accepting a maximum duration of 5 s between peaks (Fig. 2). The threshold TH_d is chosen to detect slow walking (minimum cadence around 40 steps/min, corresponding to about a stride duration of 3 s). Finally, only the walking episodes that contained at least two consecutive right and left strides (or five steps) were considered as true locomotion [40].

2.2.4 Steps and walking bouts detection using two IMU (both feet)

First, the algorithm explained in the previous sections is applied to the right and left IMUs' signals independently. Thus,

the thresholds for the peak selection obtained for the right and left foot might be slightly different to better adjust to asymmetric gait patterns. As the right and left signals are synchronized, the peaks detected on the right (ωN -LPF-CWT-right) and left (ωN -LPF-CWT-left) processed angular velocity norms are merged to obtain the right and left mid-swing events. Taken together, these events correspond to the step detection. The maximum duration accepted between peaks within the same walking period is reduced to 3.5 s [10]. Finally, the WBs are detected using the threshold TH_d adapted for step-related peaks ($TH_d = 1.5 + average(Dsteps)(s)$, with $Dsteps$ the average duration of the previous steps that belong to the current WB).

3 Validation

The performance of the WB classification was evaluated against the reference (INDIP pressure insoles) by calculating sensitivity, specificity, precision, and accuracy as follow (Eq. 2).

$$\begin{aligned} \text{sensitivity} &= \frac{TP}{TP+FN}, \text{specificity} = \frac{TN}{TN+FP} \\ \text{accuracy} &= \frac{TP+TN}{Total}, \text{precision} = \frac{TP}{TP+FP} \end{aligned} \quad (2)$$

Each binary vector is sampled at 40 Hz, and a value of 0 or 1 is assigned every second for no locomotion or locomotion, respectively. The true positives (TP), true negatives (TN), false positives (FP), and false negatives (FN) were defined by comparing the binary vector of the reference with the output of the walking detection algorithms (0: no locomotion, 1: locomotion).

4 Results

4.1 Validation & ROC curves

The mean age of the sample was 30 ± 7.2 years (range 24–46) for HY (5 women, 5 men), and 72.8 ± 3.3 years (range 69–78) for HA (3 women, 5 men). The total number of WBs reported by the INDIP system (i.e., the reference system) was 1156 with an average of (mean \pm std) 63.9 ± 33.5 and 71.4 ± 36.7 WBs for HY and HA, respectively. An

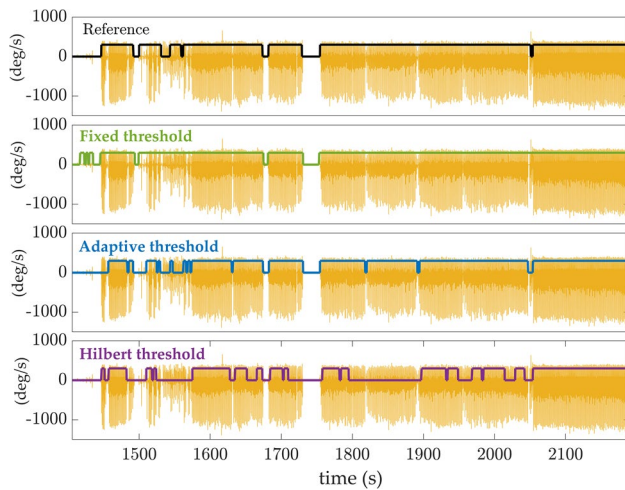


Fig. 5 Illustration of walking detection using the different thresholding methods on data recorded in one subject: *fixed* threshold (green), *adaptive* threshold (blue) and *Hilbert* threshold (purple). The reference classification, obtained from the plantar pressure of the INDIP system, is displayed in black at the top of the figure

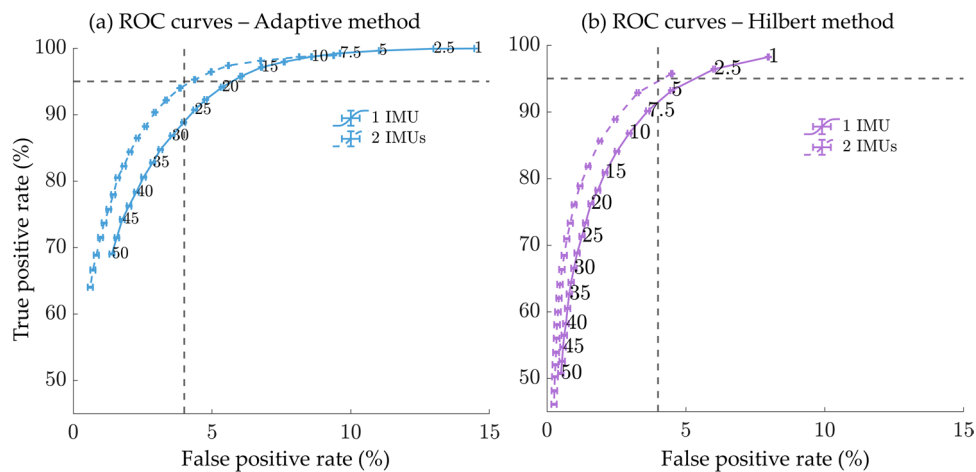


Fig. 6 ROC curves for performance evaluation as a function of percentile values from 1 to 50% when the angular velocity norm ωN is used as input. The curves are obtained by averaging the results over the 10 subjects when one IMU (continuous line) or two IMUs (dashed line) are used; **(a)** Adaptive threshold method (TH_{adapt}) based on the percentile of the obtained peak amplitude distribution

illustrative example of the walking periods detected by the proposed algorithm, using the three thresholding methods, is shown in Fig. 5. The reference classification obtained using the INDIP system is shown in black (top graph, Fig. 5). We note that the fixed threshold method recognizes all movements as WBs. In contrast, the Hilbert method (1th percentile) is much more restrictive and misclassifies certain walking periods (false negatives). In this example, the adaptive method (10th percentile) seems to provide the best walking detection.

The adaptive (TH_{adapt}) and Hilbert ($TH_{hilbert}$) methods depend on the percentile value for threshold selection. To evaluate the influence of this parameter on classification performance, we computed the ROC curves for different percentile values from 1 to 50% with 2.5% increments. Figure 6 shows the average ROC curves calculated for the 18 subjects when one IMU (one foot) or two IMUs (two feet) are used. For the adaptive (TH_{adapt}) method, the best performances are obtained for percentile values between 10% and 12.5%. A higher percentile value would result in a lower sensitivity (some WBs would not be detected). Conversely, a percentile value of less than 10% would result in an increase in the false positive rate (FPR, 1-specificity). As mentioned in the previous section, the Hilbert method ($TH_{hilbert}$) is more restrictive. The FPR is below 5% for all percentile values tested. However, the sensitivity drops sharply when the percentile value is too high (Fig. 6b). Consequently, the $TH_{hilbert}$ should be low (maximum 1%) to avoid a high number of missing walking periods. The algorithms based on two IMUs (right and left foot) demonstrate slightly higher

detected above the *fixed* threshold ($TH_{fixed} = 100^\circ/s$); **(b)** Hilbert method: The threshold ($TH_{hilbert}$) is defined as the percentile of the peak amplitude distribution in the pre-selected walking bouts. The horizontal and vertical dashed lines correspond to a 95% true positive rate and a 4% false positive rate, respectively

performances (Supplementary material A; Table 1), mainly in terms of specificity. Indeed, the ROC curves obtained with a single IMU are shifted towards a higher false positive rate as seen in Fig. 6. The same procedure was applied to the accelerometer data, and the ROC curves can be found in Supplementary material B.

Table 1 summarizes the performance obtained for one IMU and for the *fixed*, *adaptive*, and *Hilbert* methods. Based on the ROC curves, we used 10th percentile for the *adaptive* method, and 1th percentile for the *Hilbert* approach. When using the gyroscope signal as input, the *adaptive* and *Hilbert* methods yield similar results with an accuracy of $93 \pm 4\%$, precision of $76 \pm 17\%$, sensitivity of $98 \pm 2\%$, and specificity of $91.5 \pm 4\%$.

Not surprisingly, the method based on the fixed threshold is very sensitive (almost 100%), which means that all WBs are correctly detected. However, given the lower values for specificity (<70%) and precision (<90%), other movements might be misclassified as walking. In general, the results obtained when using the gyroscope signal as input show higher sensitivity and slightly lower precision compared to the acceleration signal (Table 1). Thus, using the gyroscope signal could result in a higher number of false positive WBs, but a lower number of missing walking periods (FNs).

5 Discussion

5.1 Walking detection

The walking and stride/step detection algorithms using foot IMU data performed well when applied to a challenging database of 2.5 h of free-living activities. Detection of walking based on a single foot gyroscope signal was achieved with high accuracy (>90%) and sensitivity (>98%) for the three threshold methods tested (Table 1). In addition, when adaptive thresholds were used for peak selection (i.e., *adaptive* and *Hilbert* methods),

the precision and specificity were over 75% and 91%, respectively. As expected, the results were slightly better for the configuration with two IMUs (one on each foot) because the steps are detected when the peaks from the right and left feet are combined, which is consistent with the reference system (Supplementary material A, Table 1). The algorithm, based on a single IMU, allows the detection of the mid-swing events of one foot (stride-related peaks). Consequently, we increased the maximum resting period time within a bout to 5 s, compared to 3 s when steps are detected, as we do not know if the last or first step of a bout is performed with the unquipped foot. Thus, this threshold of 5 s allows longer resting periods within a bout, and successive walking bouts might be merged together, leading to false positive detection compared to the reference system. Similar accuracy, but slightly lower sensitivity was obtained when the acceleration norm was used as input signal (Table 1).

The proposed algorithm demonstrates an efficient peak enhancement procedure and mid-swing events detection (Figs. 3, 4). As explained in the “*Algorithm implementation*” section, the detection of the mid-swing events depends on a signal amplitude threshold. The *fixed* threshold, chosen to a low value, allows high sensitivity at the expense of lower specificity. The specificity of the walking detection is considerably improved by using the two customized thresholds (*adaptive* and *Hilbert* methods). Using the 10th percentile of the peak amplitude distribution (i.e., *adaptive* method) allows to remove the peaks which most likely do not correspond to walking (Fig. 4). Regarding the *Hilbert* method, the pre-selected walking periods, based on the *Hilbert* envelope, reduce the possibility of false positive detection. This method is more restrictive than the other two (Figs. 4, 5), and the threshold based on the percentile of the peak amplitude distribution in the pre-selected bouts (i.e., $TH_{hilbert}$) should be low to avoid a high number of missing strides. Thus, the *adaptive* and *Hilbert* methods have two main advantages: first, the specificity of the walking detection is improved, and second, those thresholds are based on the data distribution without selecting a specific threshold a priori. Therefore, these methods, which are subject-specific, can be well-adapted to different populations (e.g., slow walkers versus healthy subjects). The choice of one of these threshold methods depends on the application and whether researchers prefer high specificity or high sensitivity in the walking detection. If the main goal is to evaluate the patient’s performance at home based on the distribution of walking speed during the day, we recommend using the *adaptive* or *Hilbert* methods with high specificity. However, if the goal is to focus on the amount of activity performed, it is better to

Table 1 The results of the walking detection algorithms based on one IMU (gyr: gyroscope; and acc: accelerometer) for the three different thresholding methods. The 10th percentile is used for the adaptive method, and the 1th percentile for the Hilbert approach

| | | Acc (%) mean (std) | Prec (%) mean (std) | Sen (%) mean (std) | Spe (%) mean (std) |
|------------|----------------|-----------------------|------------------------|-----------------------|-----------------------|
| Gyr | TH_{fixed} | 90.2 (4.6) | 69.5 (16.5) | 99.9 (0.0) | 84.5 (8.3) |
| | TH_{adapt} | 92.8 (3.9) | 76.1 (17.1) | 98.7 (1.7) | 91.4 (5.2) |
| | $TH_{hilbert}$ | 92.9 (3.5) | 76.2 (18.5) | 98.2 (2.3) | 76.2 (18.5) |
| Acc | TH_{fixed} | 94.7 (2.1) | 81.6 (9.8) | 96.4 (4.8) | 92.0 (5.8) |
| | TH_{adapt} | 94.9 (2.0) | 86.2 (9.5) | 91.4 (5.9) | 95.9 (2.1) |
| | $TH_{hilbert}$ | 94.4 (2.6) | 85.6 (11.2) | 91.2 (5.6) | 96.1 (2.0) |

choose a very sensitive method, as each movement can be important. In view of our results, we recommend the use of the *adaptive* method, which has the best trade-off between sensitivity and specificity and a lower computational cost than the *Hilbert* envelope calculation.

Moreover, in this study, we have shown that the gyroscope and accelerometer signals can both be used as input to the walking detection algorithm. Using the gyroscope signals is an interesting option since this allows to subsequently extract gait parameters at each walking bout using dedicated algorithms [28]. However, power consumption of the gyroscope and consequently battery life of the wearable system are critical aspects to consider when conducting long-term monitoring studies. In this context, it might be interesting to collect only accelerometer data, which is less power-consuming than a gyroscope, and characterize the gait by duration of bouts, cadence, and asymmetry if synchronized devices are used on feet.

5.2 Comparison to existing algorithms based on foot-mounted IMUs

In a recent study, Ullrich et al., implemented a novel algorithm for the detection of gait from daily-life recordings [41]. Their approach, based on frequency spectrum analysis, achieved high sensitivity (0.97) on semi-standardized gait tests and high sensitivity (0.98) and specificity (0.96) on laboratory measurements, which is comparable to our results. However, those performance were obtained when the angular rate around the media-lateral axis (considered as the best channel configuration) is used as input signal, requiring therefore a functional calibration. A sensitivity and specificity of 0.89 and 0.81 respectively were reached for the norm of the 3D rate of rotation, which underperforms our results.

Regarding stride detection, a Hidden Markov Model (HMM) approach demonstrated promising results in patients with Parkinson's disease performing in laboratory walking tests [42]. However, the performance decreased by almost 4% when applied to a free-living recorded dataset. The data-driven HMM approach is highly dependent on the walking bout length, with lower performance for bouts with less than 30 strides [42]. Since short walking bouts (less than 30 s) represent, around 65% of total strides per day [23], this drop in stride recognition performance could be a limitation in a free-living environment. The advantage of the algorithm we proposed in this study is the step- or stride-based detection before the walking detection. Thus, the performance of step/stride detection is independent of the walking bout length.

The main objective of the current study was to validate the walking bout detection method. Therefore, we did not focus on the performance of step/stride detection. However, it is worth noting that unlike the aforementioned approaches, our algorithm enables simultaneous step/stride and walking periods detection.

The outcomes of our algorithm provide sufficient information (i.e., the type of activity (locomotion versus non-locomotion), its duration, its intensity, and its frequency) to further analyze the daily physical behavior and their temporal variations [43, 44].

5.3 Strength and limitations

The strengths of this study are evidently associated to the validation of the walking detection algorithm on a challenging database using gyroscope or accelerometer data collected in a real-life like monitoring setting. In addition, the developed algorithm is based on the norm of the gyroscope or accelerometer signal. Therefore, no calibration procedure to correct the sensor orientation is necessary, which makes this algorithm very practical for real life monitoring. However, some limitations must also be acknowledged. Although participants were asked to perform various gait patterns (inside/outside, up/down stairs) to test the algorithm under different conditions, only healthy individuals were included. Therefore, the algorithm needs further validation for very slow walking or gait abnormalities in different clinical populations. One potential limitation is the robustness for very impaired walking patterns, characterized by asymmetry and/or the usage of walking aids. However, we expect our approach to be adaptable to other cohorts as long as the cyclic properties of gait are present in the signals.

Furthermore, we did not evaluate the performance of our algorithm for distinguishing walking to other activities of daily living (e.g. stairs, cycling, running, vacuuming, rope jumping etc.). Future investigations are necessary to verify the robustness of such classification.

5.4 Clinical perspectives

The WB detection methods proposed in this study open new perspectives for gait analysis in real-world conditions which is very relevant for future clinical applications. Once WBs are detected, the spatio-temporal gait parameters such as gait speed, cadence, foot clearance, stride length and variability can be extracted using an IMU (accelerometer and gyroscope) attached to the shoes [25].

The assessment of gait speed under real-life conditions, and the effects of specific interventions or medications on patient mobility are of great interest [8]. Another important clinical application of measuring the spatio-temporal gait parameters under real-world conditions is the evaluation of functional/physical fatigue during the day (i.e., termed ecological fatigue). In the laboratory, fatigue can be quantified using specific walking tests such as the 6-min walk test [45]. However, the measurement of ecological fatigue is still in its infancy and should be explored in future studies. Decreases in activity engagement, walking bout duration and gait speed over the course of the day, as measured by a foot-mounted IMU, may be an interesting direction to investigate further.

6 Conclusion

This study validated a robust algorithm for WB detection in a real-life like environment using a foot-mounted IMU. The norms of gyroscope or accelerometer signals are used as input signal to overcome the calibration procedure, which makes this algorithm very practical for real life monitoring. The best results were obtained using the *adaptive* threshold method with sensitivity and specificity of 98% and 91% respectively. For ambulatory monitoring, robust walking detection is required to complete the processing pipeline from raw recorded data to walking/ mobility outcomes. Therefore, this validated algorithm enables robust assessment of locomotion in real-world conditions, opening new perspectives. Ecological fatigue, the effects of medication or rehabilitation periods on physical activity and gait in everyday life can be further explored.

Supplementary Information The online version contains supplementary material available at <https://doi.org/10.1007/s11517-023-02826-x>.

Acknowledgements The authors would like to acknowledge all the assessors, principal investigators and members of the Mobilise-D WP2 work-package for continuous discussion and critical input. They are particularly grateful to the participants in the study for their time and enthusiastic contribution, especially during the pandemic. This research was funded by the Austrian Federal Ministry for Climate Action, Environment, Energy, Mobility, Innovation and Technology, the Federal Ministry for Digital and Economic Affairs, and the federal state of Salzburg under the research programme COMET—Competence Centers for Excellent Technologies—in the project Digital Motion in Sports, Fitness and Well-being (DiMo). This study was co-funded by the European Union’s Horizon 2020 research and innovation programme and EFPIA via the Innovative Medicine Initiative 2 (Mobilise-D project, grant number IMI22017-13-7-820820). The views expressed are those of the authors and not necessarily those of the IMI, the European Union, the EFPIA, or any Associated Partners. LA and SDD were also supported by the National Institute for Health Research (NIHR) Newcastle Biomedical Research Centre (BRC) based at Newcastle upon Tyne Hospital NHS Foundation Trust and Newcastle University, and by the NIHR/Wellcome Trust Clinical Research Facility (CRF) infrastructure at Newcastle upon Tyne Hospitals NHS Foundation Trust.

Funding Open access funding provided by EPFL Lausanne

Declarations

Ethics approval and consent to participate The study was conducted according to the Helsinki declaration, approved by the University of Sheffield Research Ethics Committee (application number 029143). All patients had written informed consent.

Conflict of interest The authors declare no competing interests.

Open Access This article is licensed under a Creative Commons Attribution 4.0 International License, which permits use, sharing, adaptation, distribution and reproduction in any medium or format, as long as you give appropriate credit to the original author(s) and the source, provide a link to the Creative Commons licence, and indicate if changes were made. The images or other third party material in this article are included in the article's Creative Commons licence, unless indicated otherwise in a credit line to the material. If material is not included in

the article's Creative Commons licence and your intended use is not permitted by statutory regulation or exceeds the permitted use, you will need to obtain permission directly from the copyright holder. To view a copy of this licence, visit <http://creativecommons.org/licenses/by/4.0/>.

References

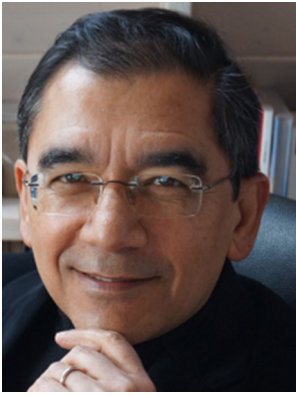
- de Bruin ED, Hartmann A, Uebelhart D, Murer K, Zijlstra W (2008) Wearable systems for monitoring mobility-related activities in older people: a systematic review. *Clin Rehabil* 22(10–11):878–895
- Vienne A, Barrois RP, Buffat S, Ricard D, Vidal PP (2017) Inertial sensors to assess gait quality in patients with neurological disorders: A systematic review of technical and analytical challenges. *Front Psychol* 8(May):817
- Taraldsen K, Chastin SFM, Riphagen II, Vereijken B, Helbostad JL (2012) Physical activity monitoring by use of accelerometer-based body-worn sensors in older adults: A systematic literature review of current knowledge and applications. *Maturitas* 71(1):13–19
- Hansen BH, Kolle E, Dyrstad SM, Holme I, Anderssen SA (2012) Accelerometer-determined physical activity in adults and older people. *Med Sci Sports Exerc* 44(2):266–272
- Middleton A, Fritz SL, Lusardi M (2015) Walking speed: The functional vital sign. *J Aging Phys Act* 23(2):314–322
- Brach JS, VanSwearingen JM, Newman AB, Kriska AM (2002) Identifying Early Decline of Physical Function in Community-Dwelling Older Women: Performance-Based and Self-Report Measures. *Phys Ther* 82(4):320–328
- Pieper C, Li T, Johnson J, and Lapuerta P (2005) “Walking speed predicts health status and hospital costs for frail elderly male veterans.” *Artic. J. Rehabil. Res. Dev*
- Atrsaei A et al (2021) “Gait speed in clinical and daily living assessments in Parkinson’s disease patients: performance versus capacity.” *npj Park Dis* 7(1):1–11
- Weiss A, Sharifi S, Plotnik M, Van Vugt JPP, Giladi N, Hausdorff JM (2011) Toward automated, at-home assessment of mobility among patients with Parkinson disease, using a body-worn accelerometer. *Neurorehabil Neural Repair* 25(9):810–818
- Paraschiv-Ionescu A, Newman C, Carcreff L, Gerber CN, Armand S, Aminian K (2019) Locomotion and cadence detection using a single trunk-fixed accelerometer: Validity for children with cerebral palsy in daily life-like conditions. *J Neuroeng Rehabil* 16(1):1–11
- Lyons GM, Culhane KM, Hilton D, Grace PA, Lyons D (2005) A description of an accelerometer-based mobility monitoring technique. *Med Eng Phys* 27(6):497–504
- Hickey A, Del Din S, Rochester L, Godfrey A (2017) Detecting free-living steps and walking bouts: Validating an algorithm for macro gait analysis. *Physiol Meas* 38(1):N1–N15
- González RC, López AM, Rodríguez-Uría J, Álvarez D, Alvarez JC (2010) Real-time gait event detection for normal subjects from lower trunk accelerations. *Gait Posture* 31(3):322–325
- Köse A, Cereatti A, Della Croce U (2012) Bilateral step length estimation using a single inertial measurement unit attached to the pelvis. *J Neuroeng Rehabil* 9(1):1–10
- Avci MMPA, Bosch S (2010) “Activity Recognition Using Inertial Sensing for Healthcare, Wellbeing and Sports Applications: A Survey,” 23th Int. Conf. Archit. Comput. Syst., p. pp.1–10
- Ganea R, Paraschiv-Ionescu A, Aminian K (2012) Detection and classification of postural transitions in real-world conditions. *IEEE Trans Neural Syst Rehabil Eng* 20(5):688–696
- Najafi B, Aminian K, Paraschiv-Ionescu A, Loew F, Büla CJ, Robert P (2003) Ambulatory system for human motion analysis

- using a kinematic sensor: Monitoring of daily physical activity in the elderly. *IEEE Trans Biomed Eng* 50(6):711–723
18. Massé F, Gonzenbach RR, Arami A, Paraschiv-Ionescu A, Luft AR, Aminian K (2015) Improving activity recognition using a wearable barometric pressure sensor in mobility-impaired stroke patients. *J Neuroeng Rehabil* 12(1):1–15
 19. Soltani A et al (2021) Algorithms for walking speed estimation using a lower-back-worn inertial sensor: A cross-validation on speed ranges. *IEEE Trans Neural Syst Rehabil Eng* 29:1955–1964
 20. Mannini A, Intille SS, Rosenberger M, Sabatini AM, Haskell W (2013) Activity recognition using a single accelerometer placed at the wrist or ankle. *Med Sci Sports Exerc* 45(11):2193–2203
 21. Shoaib M, Bosch S, Incel OD, Scholten H, and Havinga PJM (2016) “Complex Human Activity Recognition Using Smartphone and Wrist-Worn Motion Sensors,” *Sensors (Basel)*, 16, 4
 22. Soltani A, Paraschiv-Ionescu A, Dejnabadi H, Marques-Vidal P, Aminian K (2020) Real-World Gait Bout Detection Using a Wrist Sensor: An Unsupervised Real-Life Validation. *IEEE Access* 8:102883–102896
 23. Soltani A, Dejnabadi H, Savary M, Aminian K (2020) Real-World Gait Speed Estimation Using Wrist Sensor: A Personalized Approach. *IEEE J Biomed Heal Informatics* 24(3):658–668
 24. Soltani A et al (2017) Locomotion detection and cadence estimation using 3D wrist accelerometer: an in-field validation. *Gait Posture* 57:186–187
 25. Mariani B, Hoskovec C, Rochat S, Büla C, Penders J, Aminian K (2010) 3D gait assessment in young and elderly subjects using foot-worn inertial sensors. *J Biomech* 43(15):2999–3006
 26. Trojaniello D et al (2014) Estimation of step-by-step spatio-temporal parameters of normal and impaired gait using shank-mounted magneto-inertial sensors: Application to elderly, hemiparetic, parkinsonian and choreic gait. *J Neuroeng Rehabil* 11(1):1–12
 27. Dadashi F, Mariani B, Rochat S, Büla CJ, Santos-Eggimann B, Aminian K (2014) Gait and Foot Clearance Parameters Obtained Using Shoe-Worn Inertial Sensors in a Large-Population Sample of Older Adults. *Sensors (Basel)* 14(1):443
 28. Mariani B, Rouhani H, Crevoisier X, Aminian K (2013) Quantitative estimation of foot-flat and stance phase of gait using foot-worn inertial sensors. *Gait Posture* 37(2):229–234
 29. Peruzzi A, Della Croce U, Cereatti A (2011) Estimation of stride length in level walking using an inertial measurement unit attached to the foot: a validation of the zero velocity assumption during stance. *J Biomech* 44(10):1991–1994
 30. Warmerdam E et al (2020) Long-term unsupervised mobility assessment in movement disorders. *Lancet Neurol* 19(5):462–470
 31. Espay AJ et al (2019) A roadmap for implementation of patient-centered digital outcome measures in Parkinson’s disease obtained using mobile health technologies. *Mov Disord* 34(5):657–663
 32. Bourke AK, Ihlen EAF, Bergquist R, Wik PB, Vereijken B, Helbostad JL (2017) A Physical Activity Reference Data-Set Recorded from Older Adults Using Body-Worn Inertial Sensors and Video Technology—The ADAPT Study Data-Set. *Sensors* 17(3):559
 33. Salis F, Bertuletti S, Bonci T, Della Croce U, Mazzà C, Cereatti A (2021) A method for gait events detection based on low spatial resolution pressure insoles data. *J Biomech* 127:110687
 34. Salis F et al (2021) “A wearable multi-sensor system for real world gait analysis,” *Proc. Annu. Int. Conf. IEEE Eng. Med. Biol. Soc. EMBS*, pp. 7020–7023. <https://www.frontiersin.org/articles/10.3389/fbioe.2023.1143248/abstract>
 35. Moufawad el Achkar C, Lenoble-Hoskovec C, Paraschiv-Ionescu A, Major K, Büla C, Aminian K (2016) Instrumented shoes for activity classification in the elderly. *Gait Posture* 44:12–17
 36. Paraschiv-Ionescu A, Newman CJ, Carcreff L, Gerber CN, Armand S, Aminian K (2019) “Correction: Locomotion and cadence detection using a single trunk-fixed accelerometer: Validity for children with cerebral palsy in daily life-like conditions. *J Neuroeng Rehabil* 16(1):1–11. <https://doi.org/10.1186/s12984-019-0494-z>
 37. Shao X, Ma C (2003) A general approach to derivative calculation using wavelet transform. *Chemom Intell Lab Syst* 1–2(69):157–165
 38. Greene BR, Foran TG, McGrath D, Doheny EP, Burns A, Caulfield B (2012) A comparison of algorithms for body-worn sensor-based spatiotemporal gait parameters to the gaitrite electronic walkway. *J Appl Biomech* 28(3):349–355
 39. Paraschiv-Ionescu A, Soltani A, Aminian K (2020) “Real-world speed estimation using single trunk IMU: Methodological challenges for impaired gait patterns.” *Proc Annu Int Conf IEEE Eng Med Biol Soc EMBS 2020*:4596–4599
 40. Kluge F et al (2021) Consensus based framework for digital mobility monitoring. *PLoS ONE* 16(8):e0256541
 41. Ullrich M et al (2020) “Detection of Gait from Continuous Inertial Sensor Data Using Harmonic Frequencies,” *XX (XX)*, 1–10
 42. Roth N et al (2021) “Hidden Markov Model based stride segmentation on unsupervised free-living gait data in Parkinson’s disease patients,” *J Neuroeng Rehabil*, 18, 1
 43. Paraschiv-Ionescu A et al (2018) Concern about Falling and Complexity of Free-Living Physical Activity Patterns in Well-Functioning Older Adults. *Gerontology* 64(6):603–611
 44. Paraschiv-Ionescu A, Perruchoud C, Buchser E, and Aminian K (2012) “Barcoding Human Physical Activity to Assess Chronic Pain Conditions,” *PLoS One*, 7, 2
 45. Murphy SL, Kratz AL, Niemiec SLS (2017) Assessing Fatigability in the Lab and in Daily Life in Older Adults With Osteoarthritis Using Perceived, Performance, and Ecological Measures. *Journals Gerontol Ser A* 72(1):115–120

Publisher’s note Springer Nature remains neutral with regard to jurisdictional claims in published maps and institutional affiliations.



Gaëlle Prigent is a PhD student at EPFL. Her research focuses on physical activity monitoring within clinical populations, and the development of algorithms to quantify physical activity in real-world conditions using wearable sensors.



Kamiar Aminian is a Professor of medical instrumentation at EPFL. His research focuses on methodologies for human movement monitoring and analysis in real-world conditions mainly based on wearable technology.



Tecla Bonci is a biomedical engineer and research associate in biomechanics. Her research focuses on human movement biomechanics with interests in increasing the resolution of human movement analysis performed using stereophotogrammetry as well as in various modelling techniques that can improve the insight into individuals' motor capacity and performance.



Andrea Cereatti is a Professor of Bioengineering. His research focuses on the biomechanics of human movement and on the definition of methods, modelling techniques and protocols that improved the insight into human motor function and allow for the clinical assessment of individual's motor capacity and performance.



Kirsty Scott (MSc) is a research associate in biomechanics at the University of Sheffield. Her focus is on the analysis of human movement within clinical populations and the development of wearable devices to quantify real-world mobility.



Francesca Salis is a PhD student. Her research focuses on the optimization and development of methods for spatial-temporal parameters estimation to assess gait performances in real-world scenarios, using wearable technologies.



Claudia Mazzà is a Professor of Biomechanics. Her research focuses on the biomechanics of human movement and on the definition of experimental and modelling techniques for the clinical assessment of an individual's locomotor and postural abilities.



Lisa Alcock is a Senior Research Associate and Gait lab manager at Newcastle University with extensive expertise in gait analysis for clinical applications.



Clint Hansen is the deputy head of the Neurogeriatrics Research group Kiel and his research focuses on understanding and characterizing the biomechanics of human movement in health and disease. This process is facilitated through 3D Motion capture, EMG, IMU, GPS analyses and musculoskeletal modeling.



Silvia Del Din is a Newcastle University Academic Track Fellow. Her translational research interests focus on digital health for enhancing remote monitoring and clinical management in ageing and neurodegeneration.



Anisoara Paraschiv-Ionescu is a scientist at EPFL. Her research interests are modeling human physical activity patterns in health and disease to provide objective assessment of medical interventions.



Eran Gazit has M.Sc in electronic engineering and M.Sc in Biomedicine from Tel-Aviv University, Tel-Aviv, Israel. He works in the Center for the Study of Movement, Cognition, and Mobility as an algorithm and system developer. His research area includes cognitive and motor function, their changes with aging and disease (e.g., Parkinson's disease, multiple sclerosis), and the development of new tools and methods for gait analysis from wearable devices.